

# Spin-LbL Assembled Coatings of SiO<sub>2</sub> and TiO<sub>2</sub> oppositely Charged Nanoparticles for Superhydrophilicity, Antifogging and Antireflection

Fusheng Yang<sup>1,2\*</sup>, Peng Wang<sup>1</sup>, Xiaoli Yang<sup>2</sup>, Zaisheng Cai<sup>1\*</sup>

<sup>1</sup>College of Chemistry, Chemical Engineering and Biotechnology, Donghua University, Shanghai 201620, China

<sup>2</sup>Anhui Polytechnic University, Wuhu 241000, China

\* Authors contributed equally

**\*Corresponding author:** Fusheng Yang, College of Chemistry, Chemical Engineering and Biotechnology, Donghua University 2999, North Renmin Road, Songjiang District, Shanghai, 201620, China, Tel: 86-21-67792808; E-mail: [eyangfs@sina.com](mailto:eyangfs@sina.com)  
Zaisheng Cai, College of Chemistry, Chemical Engineering and Biotechnology, Donghua University, 2999, North Renmin Road, Songjiang District, Shanghai, 201620, China, Tel: 86-21-67792609; E-mail: [zshcaidh@sina.com](mailto:zshcaidh@sina.com)

## Abstract

Superhydrophilic, Antifogging (AF) and Anti-Reflective (AR) coatings were fabricated via layer-by-layer spin coating assembly of oppositely charged Nanoparticles (NPs) followed by calcination. The positively charged TiO<sub>2</sub> NPs (+ 40.8 mV) and negatively charged SiO<sub>2</sub> NPs (-41.5 mV) were bound firmly together via electrostatic interaction. The resultant coatings can obtain excellent properties using only three bi layers of alternating the TiO<sub>2</sub> NPs and SiO<sub>2</sub> NPs. The coatings exhibited excellent AF properties due to the super hydrophilicity of the coating, revealed excellent AR properties (> 95.2%) due to the low refractive index coating and an appropriate coating thickness, and showed excellent super hydrophilic properties (~ 0°, < 0.2 s) due to a nano-roughness structure. The calcination temperature between 400 and 550 °C has little effect on the transmittance of the coatings. In addition to being environmentally friendly, the simple, cost-efficient and green fabrication process made the superhydrophilic, AF and AR coatings have various applications in optical instruments and display devices.

**Keywords:** Spin-coating; Layer-by-layer assembly; Superhydrophilicity; Antifogging; Antireflection

## Introduction

Fogging is due to the condensation of discrete and dispersed light-diffusing tiny droplets when the temperature of a material surface is below the dew point of the vapor<sup>[1,2]</sup>. The fogging phenomenon is quite common and often causes trouble to people in everyday life. To solve the problem, we can fabricate a coating, which is wet by water completely and instantaneously (superhydrophilic state: water contact angle < 5° within 0.5 s or less)<sup>[3,4]</sup>. To obtain a highly transparent surface, we should develop antireflective (AR) coatings<sup>[5-7]</sup>. The coatings which can effectively enhance the transmission of light have attracted intensive interest because they are indispensable for almost

all kinds of optical and display devices. The basic principle of antireflection that was presented by Fresnel<sup>[8]</sup>, is the destructive interference between light reflected from the coating-substrate and the air-coating interfaces. Generally, an ideal AR coating should meet the following two conditions<sup>[8]</sup>: (1)  $n_c = (n_a \times n_s)^{1/2}$ , where  $n_c$ ,  $n_a$  and  $n_s$  are the refractive indices of the coating, the air ( $n_a = 1.00$ ) and the substrate, respectively. (2)  $d = \lambda/4n_c$ ,  $d$  is the thickness of the coating,  $\lambda$  is the wavelength of incident light. Reflection will be suppressed at the wavelength near the quarter-wavelength optical thickness (quarter-wave coating). For a glass substrate ( $n_s = 1.5$ ), the refractive index of AR coating should be ca. 1.22<sup>[6,9]</sup>. Since no existing bulk material possesses such a low refractive index, nanopores (nanomaterials) are in-

Received date: May 24, 2017

Accepted date: July 17, 2017

Published date: July 20, 2017

**Citation:** Yang, F., et al. Spin-LbL Assembled Coatings of SiO<sub>2</sub> and TiO<sub>2</sub> oppositely Charged Nanoparticles for Superhydrophilicity, Antifogging and Antireflection. (2017) J Nanotech Mater Sci 4(2): 48- 52.

DOI: 10.15436/2377-1372.17.1552



roduced into the coating to reduce the refractive index of the coating. Therefore, as a substitute, the highly porous structure films can be used as AR coatings.

Electrostatic layer-by-layer (LbL) assembly has proven to be a simple, green and effective method to produce various kinds of coatings<sup>[10-12]</sup>. It can provide sufficient control over the thickness (in nanoscales) and structure of the coating to obtain AR properties, and therefore, wavelengths for maximum transmittance (antireflection) can be turned over the entire visible region by simply controlling the number of deposited bilayers. Dip-LbL, Spray-LbL and Spin-LbL are often used to produce various ultra-thin coatings<sup>[7,10,13]</sup>. However, the drawback of Dip-LbL is time consuming; Spray-LbL is difficult to control the uniformity of a coating thickness. As a comparison, Spin-LbL can greatly reduce the consumption of the circle time and material, meanwhile high-speed substrate rotation can also shorten the drying time. For this reason, we have employed a Spin-LbL assembly method to rapidly produce thin Antifogging (AF) and AR coatings<sup>[13]</sup>. So far, various materials have been used as AF and AR materials, eg., SiO<sub>2</sub>, TiO<sub>2</sub>, MgF<sub>2</sub>, Al<sub>2</sub>O<sub>3</sub>, ZnO, ZrO<sub>2</sub>, MgO, etc. Among them, SiO<sub>2</sub> and TiO<sub>2</sub> are better choice for AF and AR coatings<sup>[3,10]</sup>. Therefore we used them as building blocks for fabricating the coatings. SiO<sub>2</sub> and TiO<sub>2</sub> are typical optical coating materials which show high transparency and low absorption in the visible region (380 - 780 nm). Furthermore, they are known as safe, cost-efficient, abundant, and eco-friendly materials with thermal, chemical and mechanical stability. Thus, they are used practically in all fields of science and engineering.

In this work, we demonstrate that the superhydrophilic, AF and AR coatings can be readily and quickly fabricated via Spin-LbL self-assembly of the negatively charged SiO<sub>2</sub> and positively charged TiO<sub>2</sub> NPs. The layers are bound firmly together via electrostatic interaction. The resultant coatings presented excellent AF properties due to the superhydrophilicity of the coating<sup>[4]</sup>, exhibited excellent AR properties due to the low refractive index coating and an appropriate coating thickness<sup>[6]</sup>, and showed excellent superhydrophilic properties due to a rough surface.

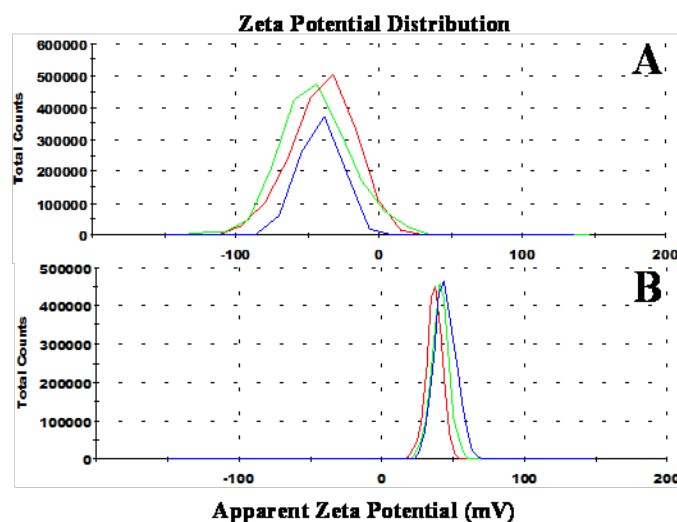
## Experimental Section

The zeta potential and particle size of SiO<sub>2</sub> and TiO<sub>2</sub> were measured in triplicate using a Zetasizer Nano ZS (Malvern instruments, UK) at 25 °C. Surface morphology and cross-section of the coatings were studied using a field-emission scanning electron microscope (FE-SEM, Hitachi S-4800) operated at an acceleration voltage of 5 kV. Transmission spectra in the range of 350 - 800 nm were recorded using a U-3310 UV-Vis spectrophotometer (Hitachi Co. Ltd. Japan) at a Relative Humidity (RH) of ca. 30%. Water Contact Angles (WCA) was performed at ca. 20 °C using a Krüss DSA 30 (Krüss GmbH, Hamburg, Germany). A water droplet of 3 µL was dropped carefully onto the sample, and the spreading process was recorded by a CCD camera, once the water droplet contacted the sample surface, the machine began to take photographs at 25 frames/s, Antifogging properties were evaluated by two methods. One was a boiling test<sup>[2]</sup>, the samples were placed on the top of a beaker containing boiling water (80 % full), and vapor condensed on the coating surface was observed and photographed. The other was a low temperature antifogging test, the samples were stored in a freez-

er at -15 °C for 3 h and then exposed to humid air (ca. 20 °C and 65% RH) simultaneously to observe whether the fog was formed on the coating.

Glass microscope slides (SAIL BRAND Cat.No.7101) were immersed in a piranha solution (7/3 v/v of 98 wt % H<sub>2</sub>SO<sub>4</sub>/30 wt % H<sub>2</sub>O<sub>2</sub>) for 6 hours, then rinsed with ultrapure water and ethanol, and then blown dry under nitrogen. The cleaned glass slides were obtained and they were used as substrates in all experiments.

Monodisperse SiO<sub>2</sub> NPs [ca. 42 nm; Polydispersity Index (PDI) = 0.050; -41.5 mV zeta potential; measured by Zetasizer Nano-ZS] were prepared according to the literature<sup>[2,14]</sup>. TiO<sub>2</sub> NPs (ca. 8 nm in size; + 40.8 mV zeta potential; measured by Zetasizer Nano-ZS) were prepared with reference to the literature<sup>[2,15]</sup>. The superhydrophilic, AF and AR coatings were fabricated using a Spin-LbL assembly process, and this process is driven by electrostatic interaction between the positively charged TiO<sub>2</sub> NPs and negatively charged SiO<sub>2</sub> NPs. The concentration of both SiO<sub>2</sub> and TiO<sub>2</sub> NPs solution was 0.8 mg/mL. A glass substrate was held on a vacuum chuck. The negatively charged SiO<sub>2</sub> solution (-41.5 mV, see Figure 1A) and positively charged TiO<sub>2</sub> (+ 40.8 mV, see Figure 1B) were alternately spin-coated on the substrate, first at 40 rpm for 10 s and then at 2500 rpm for 20 s in succession. The process was repeated until the desired number of bilayers (coating thickness) was achieved. The other side of the glass substrate was treated in the same way as above. Finally the as-prepared coatings were calcined (heating rate: 2 °C/min) in a muffle furnace for 2.5 hours to remove organics and improve their adhesion to the substrate. They were then subsequently cooled down to room temperature (cooling rate: 3 °C/min).



(We only have the original graph. We cannot get the table from the software of the Zetasizer Nano-ZS instrument.)

**Figure 1:** Zeta potential graphs of (A) SiO<sub>2</sub> NPs (mean value: -41.5 mV) and (B) TiO<sub>2</sub> NPs (mean value: + 40.8 mV).

## Results and Discussion

To evaluate the effects of the number of deposited bilayers on the transmittance and superhydrophilicity of the coatings, we prepared a series of coatings that contained 1, 2, 3 and 4 bilayers of SiO<sub>2</sub>/TiO<sub>2</sub> coatings. Figure 2A shows the

transmission spectra of SiO<sub>2</sub>/TiO<sub>2</sub> coatings calcined at 520 °C with different deposited bilayers on glass substrates. With the increase of the number of deposited bilayers, the average transmittances in the visible range (380 - 780 nm) increase to ca. 92.7 %, 94.3 %, 95.3 % and 95.5 %, respectively. The transmittance values increase significantly compared with the bare glass (90.6 %), and this also showed that they all had excellent AR performance. The increase of transmittance may be attributed to the coating thickness (quarter-wave coating)<sup>[6]</sup> and the nanoporosity structure (low refractive index). When the transmittance value increases to 95.3% (three bilayers), the thickness of the coating is near the quarter-wave coating (ca. 140 nm, see Figure 3B), and therefore there is little increase in transmittance (0.2 %) for four bilayers. In Figure 3A (SiO<sub>2</sub>/TiO<sub>2</sub> coatings) and Figure 3C (TiO<sub>2</sub>/SiO<sub>2</sub> coatings), the different size of two kinds of NPs can be seen clearly, which increase the nano-roughness and porosity of the surface. It should be noted that SiO<sub>2</sub> NPs are much easier to adhere to glass slide and one another. The surface roughness is believed to affect the transmittance of the coatings, by closely stacking of the SiO<sub>2</sub> and TiO<sub>2</sub> NPs, nanoporosity is introduced to reduce the refractive index of the coating. When the refractive index is 1.22, the wavelength of maximum suppression is determined by the quarter-wave optical thickness of the coating. The quarter-wave coating, in turn, can be turned over the whole visible region by simply controlling the number of deposited bilayers. As seen in Figure 2A, only three bilayers can achieve a good AR coating, the average optical transmittance in the range between 380 and 780 nm was estimated to be ca. 95.3 %. In the WCA test, all the coatings of different deposited bilayers exhibited excellent superhydrophilicity (almost 0°, less than 0.2 seconds). This was due to the rough structure surface.

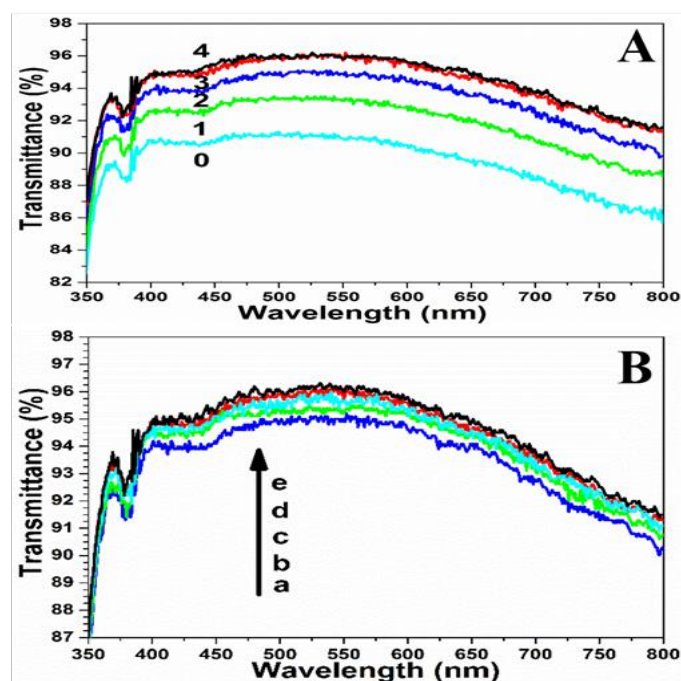


**Figure 2:** UV-Vis transmission spectra of (A) SiO<sub>2</sub>/TiO<sub>2</sub> coatings on a glass substrate with 1-4 deposited bilayers, and a bare glass (0) provided for comparison; (B) SiO<sub>2</sub>/TiO<sub>2</sub> coatings on a glass substrate with different calcination temperatures; a (400), b (450), c (500), d (520), and e (550 °C).

To assess the effects of calcination temperatures on

the transmittance and superhydrophilicity of the coatings, we prepared a series of SiO<sub>2</sub>/TiO<sub>2</sub> coatings with three deposited bilayers, which were calcined in a muffle furnace at 400, 450, 500, 520, and 550 °C for 2.5 hours. The temperature more than ca. 550 °C can make the glass thermal deformation. Figure 2B shows the transmittance values of different calcination temperatures, the average transmittance values were ca. 94.5 %, 94.9 %, 95.1 %, 95.3 % and 95.5 %, respectively. No apparent difference in transmittance (less than 1.0 %, from 94.5 % to 95.5 %) was observed when the temperature was increased from 400 to 550 °C. This is due to no change in coating thickness, because the high-temperature calcination (> 400 °C) could burn out organics and impurities of the substrate surface. For rapid and high-efficiency preparation, the temperature of 520 °C was chosen as an optimum temperature in the following experiments. In the WCA test, all the coatings of different calcination temperatures showed excellent superhydrophilic properties (almost 0°, less than 0.2 seconds).

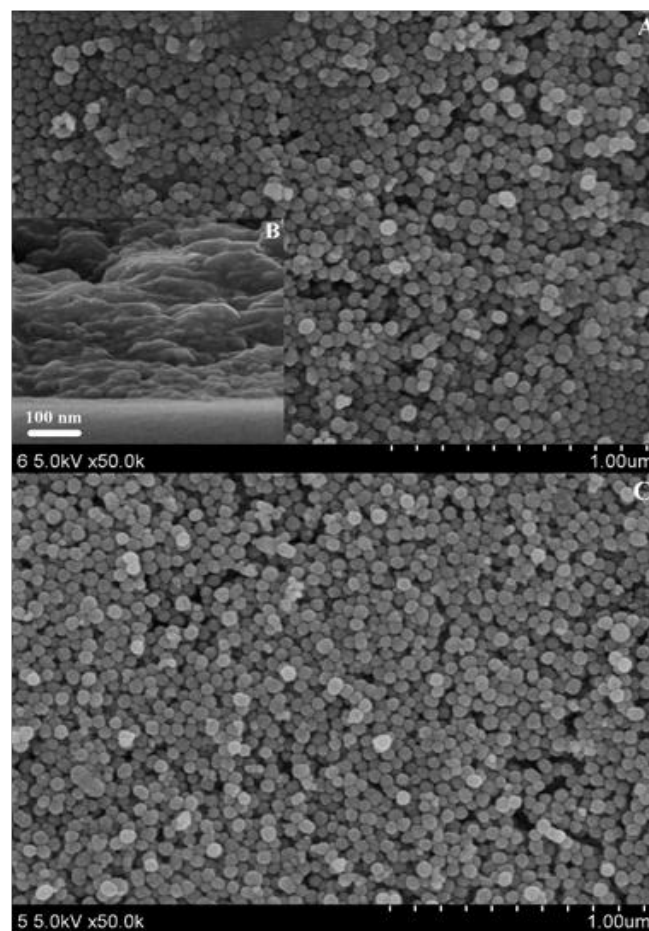


**Figure 3:** SEM images of top view (A) and cross-section view (B) of SiO<sub>2</sub>/TiO<sub>2</sub>; and top view (C) of TiO<sub>2</sub>/SiO<sub>2</sub> coatings on a glass substrate with three deposited bilayers.

The SiO<sub>2</sub>/TiO<sub>2</sub> coatings were produced as the SiO<sub>2</sub> coating was the first layer, after three deposited bilayers on both sides, the SiO<sub>2</sub>/TiO<sub>2</sub> coatings were then calcined at 520 °C for 2.5 hours. For comparison, the TiO<sub>2</sub>/SiO<sub>2</sub> coatings (the TiO<sub>2</sub> coating was the first layer) were also produced under the same conditions. The results showed that the SiO<sub>2</sub>/TiO<sub>2</sub> coatings (95.3 % in transmittance) and TiO<sub>2</sub>/SiO<sub>2</sub> coatings (95.2 %) had the same AR effect. This is because they were the same thickness

(ca. 140 nm), the number of TiO<sub>2</sub> NPs (small size) in the coating was small, and the major superhydrophilic contributor was SiO<sub>2</sub> NPs (large size). TiO<sub>2</sub> NPs were used to increase nanoporosity and nano-roughness. However, all SiO<sub>2</sub> NPs coatings are more prone to cracks. SiO<sub>2</sub> and TiO<sub>2</sub> coatings have few cracks.

The textured surfaces and void fraction can significantly enhance the wettability of surfaces with water. And this may result in enhanced AF properties. The superhydrophilic, AF properties of both SiO<sub>2</sub>/TiO<sub>2</sub> and TiO<sub>2</sub>/SiO<sub>2</sub> coatings (three bilayers) were investigated using the WCA test, boiling test and low temperature AF test.

In the WCA test, the SiO<sub>2</sub>/TiO<sub>2</sub> and TiO<sub>2</sub>/SiO<sub>2</sub> coatings were all superhydrophilic (almost 0°, less than 0.2 seconds). The spreading process of a water droplet was recorded by a CCD camera. As soon as the first water droplet contacted the coatings surface, it spread flat instantaneously to form a thin sheet-like water membrane in less than 0.2 seconds. Figure 4 is 12 consecutive screenshots of the coatings from the video, and it means that the coating is exhibiting superhydrophilicity.

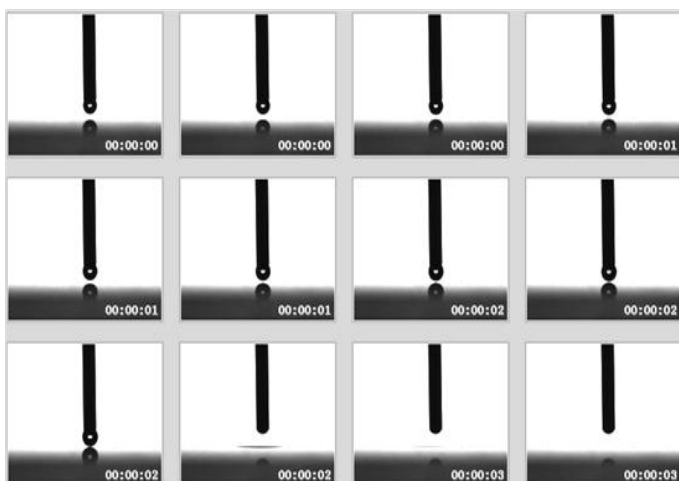


**Figure 4:** Still images captured from video recordings for a water droplet (3 µL) spreading on a substrate covered with superhydrophilic, anti-fogging and antireflective coatings.

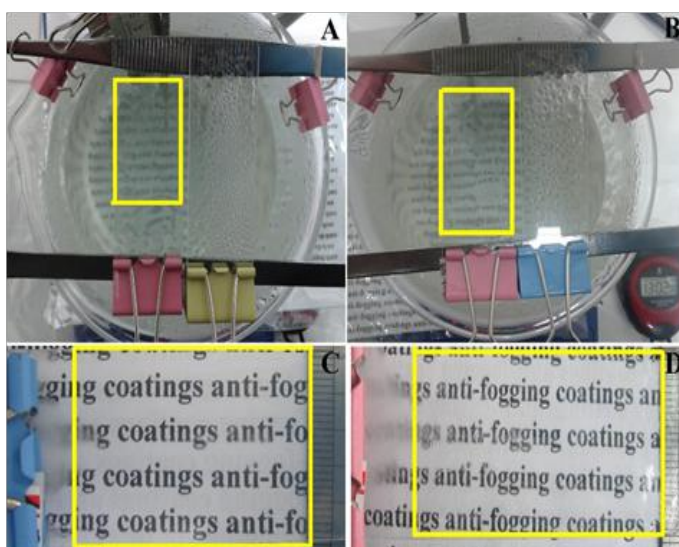


**Figure 5:** Photo images of the boiling test, (A) SiO<sub>2</sub>/TiO<sub>2</sub> and (B) TiO<sub>2</sub>/SiO<sub>2</sub> coatings. Photo images of substrates coated with (C) SiO<sub>2</sub>/TiO<sub>2</sub> and (D) TiO<sub>2</sub>/SiO<sub>2</sub> coatings after being stored at -15 °C for 3 hours in a freezer. The yellow-lined area indicates where the coating was applied.

In the boiling test, the SiO<sub>2</sub>/TiO<sub>2</sub> (Figure 5A) and TiO<sub>2</sub>/SiO<sub>2</sub> (Figure 5B) samples showed excellent AF properties. The coated slides (yellow wireframe) always remained visible; the words at the bottom of the beaker remained visible. In sharp contrast, nothing can be seen through the bare glass slide (the yellow clips for Figure 5A and the blue clips for Figure 5B). The experiment was maintained for 6 hours, the results confirmed that SiO<sub>2</sub>/TiO<sub>2</sub> and TiO<sub>2</sub>/SiO<sub>2</sub> coatings have excellent AF performance. This is because the nearly instantaneous, sheet-like wetting by water prevents light scattering water droplets from forming on the substrate surface.

In the low temperature AF test, the SiO<sub>2</sub>/TiO<sub>2</sub> (Figure 5C) and TiO<sub>2</sub>/SiO<sub>2</sub> samples (Figure 5D) showed excellent low temperature AF properties. The uncoated areas covered with frost and the words below are invisible due to strong light scattering. In sharp contrast, the coated area (yellow wireframe) can remain highly transparent and the words below can be seen clearly, because the superhydrophilic surface can prevent the formation of light-scattering tiny ice droplets which are capable of scattering light randomly on a surface.

The results of all tests confirmed that both SiO<sub>2</sub>/TiO<sub>2</sub> and TiO<sub>2</sub>/SiO<sub>2</sub> coatings exhibited excellent superhydrophilic, AF and AR properties due to the nano-roughness surface and nano-voids.

## Conclusions

In summary, superhydrophilic, antifogging and antireflective coatings can be easily fabricated from Spin-LbL assembled film of the positively charged TiO<sub>2</sub> NPs (+ 40.8 mV) and negatively charged SiO<sub>2</sub> NPs (-41.5 mV). They are bound firmly together via electrostatic interaction. This film consisted of applying three bilayers of alternating oppositely charged NPs. Calcinations at high temperature can promote the formation of stable siloxane bridges, enhance mechanical stability and adhesion to the glass substrate, and introduce 3D nanoporous networks in the coating along with enhanced hydrophilicity. The calcination temperature between 400 and 550 °C has little effect on the transmittance of the coatings. The coatings showed excellent AF properties due to the superhydrophilicity of the coating, exhibited excellent AR properties (> 95.2%) due to the low refractive index coating and an appropriate coating thickness, and showed excellent superhydrophilic properties (~ 0°, < 0.2 seconds) due to a nano-roughness structure. In addition to being environmentally friendly, the low-cost and green fabrication process made the superhydrophilic, AF and AR coatings have very promising applications in various optical devices.

**Conflict of Interest:** The authors declared no conflict of interest.

## References

1. Nuraje, N., Asmatulu, R., Cohen, R.E., et al. Durable antifog films from layer-by-layer molecularly blended hydrophilic polysaccharides. (2011) *Langmuir* 27(2): 782-791.  
[Pubmed](#) | [Crossref](#) | [Others](#)
2. Yang, F., Wang, P., Yang, X., et al. Antifogging and anti-frosting coatings by Dip-layer-by-layer self-assembly of just triple-layer oppositely charged nanoparticles. (2017) *Thin Solid Films* 634: 85-95.  
[Pubmed](#) | [Crossref](#) | [Others](#)
3. Cebeci, F.Ç., Wu, Z., Zhai, L., et al. Nanoporosity-driven superhydrophilicity: a means to create multifunctional antifogging coatings. (2006) *Langmuir* 22(6): 2856-2862.  
[Pubmed](#) | [Crossref](#) | [Others](#)
4. Xu, L., He, J. Antifogging and antireflection coatings fabricated by integrating solid and mesoporous silica nanoparticles without any post-treatments. (2012) *ACS applied materials & interfaces* 4(6): 3293-3299.  
[Pubmed](#) | [Crossref](#) | [Others](#)
5. Tahk, D., Kim, T.I., Yoon, H., et al. Fabrication of antireflection and antifogging polymer sheet by partial photopolymerization and dry etching. (2010) *Langmuir* 26(4): 2240-2243.  
[Pubmed](#) | [Crossref](#) | [Others](#)
6. Buskens, P., Burghoorn, M., Mourad, M.C.D., et al. Antireflective coatings for glass and transparent polymers. (2016) *Langmuir* 32(27): 6781-6793.  
[Pubmed](#) | [Crossref](#) | [Others](#)
7. Lu, X., Wang, Z., Yang, X., et al. Antifogging and antireflective silica film and its application on solar modules. (2011) *Surface and coatings technology* 206(6):1490-1494.  
[Pubmed](#) | [Crossref](#) | [Others](#)
8. Macleod, H.A. Thin-film optical filters. (2001) CRC press.  
[Pubmed](#) | [Crossref](#) | [Others](#)
9. Zhang, X-T., Sato, O., Taguchi, M., et al. Self-cleaning particle coating with antireflection properties. (2005) *Chemistry of Materials* 17(3): 696-700.  
[Pubmed](#) | [Crossref](#) | [Others](#)
10. Richardson, J.J., Cui, J., Björnalm, M., et al. Caruso. Innovation in Layer-by-Layer Assembly. (2016) *Chemical Reviews* 116(23): 14828-14867.  
[Pubmed](#) | [Crossref](#) | [Others](#)
11. Zhang, S., Vleminck, C., Ramirez Wong, D.D., et al. Nanopapers of layer-by-layer nanotubes. (2016) *Journal of Materials Chemistry B* 4(47): 7651-7661.  
[Pubmed](#) | [Crossref](#) | [Others](#)
12. Decher, G. Fuzzy nano assemblies: toward layered polymeric multi composites. (1997) *science* 277(5330): 1232-1237.  
[Pubmed](#) | [Crossref](#) | [Others](#)
13. Zhang, L., Lü, C., Li, Y., et al. Fabrication of biomimetic high performance antireflective and antifogging film by spin-coating. (2012) *J Colloid Interface Sci* 374(1): 89-95.  
[Pubmed](#) | [Crossref](#) | [Others](#)
14. Stöber, W., Fink, A., Bohn, E. Controlled growth of monodisperse silica spheres in the micron size range. (1968) *Journal of colloid and interface science* 26(1): 62-69.  
[Pubmed](#) | [Crossref](#) | [Others](#)
15. Hu, M.Z.-C., Harris, M.T., Byers, C.H. Nucleation and growth for synthesis of nanometric zirconia particles by forced hydrolysis. (1998) *Journal of colloid and interface science* 198(1): 87-99.  
[Pubmed](#) | [Crossref](#) | [Others](#)